Journal of Rare Cardiovascular Diseases

ISSN: 2299-3711 (Print) | e-ISSN: 2300-5505 (Online)



RESEARCH ARTICLE

Anticancer Activity of Silver Nanoparticles of Blumea Lacera and Corydalis Govaniana Against Human Skin Cancer Cells.

Md Tanweer Ahmed^{1*}, Mohit Shrivastava¹ and Md Naushad Alam²

1School of Pharmacy and Sciences, Singhania University, Pacheri Bari, Jhunjhunu - 333515, Rajasthan, India ²BBS Institute of Pharmaceutical and Allied Sciences, Plot No. 33, Knowledge Park III, Greater Noida, UP, India.

*Corresponding Author Md Tanweer Ahmed (tnwirahmd@gmail.com)

Article History

Received: 10.07.2025 Revised: 14.07.2025 Accepted: 05.08.2025 Published: 08.09.2025

Abstract: Skin cancer is among the most prevalent malignancies globally, distinguished by its aggressive and rapid proliferation. Squamous cell carcinoma is particularly concerning due to its invasive behaviour, which often leads to metastasis and can be fatal in severe cases. Current treatments for melanoma include surgical intervention, chemotherapy, radiation therapy, biological therapy, and targeted therapeutic approaches. Recent advancements in cancer treatment have increasingly explored the natural pharmaceuticals, aiming to enhance therapeutic outcomes. An annual herbaceous plant, Blumea lacera (BL)., a member of the Asteraceae family and Corydalis govaniana (CG) of family Fumariaceae were envisaged against melanoma due to their anticancer activity. Conventional system has been modified to novel drug delivery system to avoid the demerits such as low bioavailability, first pass metabolism, frequent dosing, excessive excretion of drug. Silver nanoparticles are promising nanoparticles because of their cite specific action, size and stability. Silver nanoparticles are prepared using green synthesis and optimized by Box Behnken design utilising AgNO₃ concentration (mM, X_1), microwave power (Watt, X_2), and extract concentration (X_3) as independent variable and the dependent variables, silver nanoparticle size (Y1) and absorbance (Y2). The particle size and PDI were found to be satisfactory which were 153.76 \pm 5.87 nm and PdI 0.23 \pm 0.042 respectively. zeta potential was found to be -23.961 \pm 4.66 mV which validates the stability of the formulation. In vitro drug release showed the sustained release pattern when compared to drug suspension and followed Higuchi model. From ex vivo permeation study, it was found that drug loaded silver nanoparticles showed percentage permeation of 75.08 \pm 4.34% for BL and 76.49 \pm 3.44% for CG. Antioxidant study revealed both the drugs to be highly antioxidant and comparable to ascorbic acid which was taken as a standard. MTT assay revealed that both the drugs have cytotoxic effects with Corydalis govaniana to have stronger cytotoxic effect. The results of drug loaded silver nanoparticles were found to be satisfactory and promising to be taken into account for further studies.

Keywords: Anticancer, Silver Nano Particle, MTT Assay, Blumea lacera and Corydalis govaniana.

INTRODUCTION

Skin cancer is one of the most common malignancies worldwide and is characterized by its rapid proliferation (Apalla et al. 2017). Basal cell carcinoma and squamous cell carcinoma are the most frequently diagnosed nonmelanoma skin cancers (NMSCs), in addition to melanoma (Afaq 2011). Squamous cell carcinoma is highly malignant due to its invasive nature, which can result in metastasis and, in the worst-case scenario, death (Cohen 2010). The American Cancer Society anticipates that approximately 100,640 new cases of melanoma will be diagnosed in the United States in 2024. Of these, 59,170 cases will be diagnosed in men and 41,470 cases in women. Tragically, an approximated 8,290 individuals, including 5,430 men and 2,860 women, are expected to succumb to melanoma (Anon n.d.). India is responsible for over 8% of the global cancer burden, with a mortality rate of approximately 6%, according to a recent assessment by the World Health Organization (WHO) (Ferlay et al. 2018). Melanoma is currently treated with surgery, chemotherapeutics, radiation, biological therapy, and targeted therapy (Mangione et al. 2023).

Researchers are investigating strategies that circumvent fixed doses, rapid titration, and inflexible designs in

order to enable individualized drug adjustment for various patients, thereby overcoming the constraints of monotherapy (Sohrabi et al. 2022). The elimination of both healthy and malignant cells is the consequence of monotherapy approaches, indiscriminately attack actively proliferating cells (Yap et al. 2013). Recent research has focused on the integration of synthetic and natural pharmaceuticals in the field of cancer therapy. This method provides numerous advantages, such as the ability to target a variety of cancer pathways, reduce toxicity, and employ a personalized treatment plan to enhance efficacy. Furthermore, combination therapy has the capacity to simultaneously induce cytotoxic effects on cancer cells and reduce the detrimental effects on healthy cells (Mokhtari et al. 2017).

An annual herbaceous plant, Blumea lacera (BL)., is a member of the Asteraceae family. It contains a diverse spectrum of phytochemicals that have significant therapeutic potential. This herb, which is also known as kukkuradru in Sanskrit and Karanda jangli muli in Hindi, is cultivated for its use in sustenance, essential oil processing, and a variety of ethnomedical applications. These phytochemicals demonstrate a diverse array of pharmacological properties, including antipyretic, anti-inflammatory, anthelmintic, diuretic, antidiarrheal,

antimicrobial, cytotoxic, astringent, liver-protective properties, a relaxant, anxiolytic, antiviral, analgesic, anticancer, hypothermic, anti-bacterial, antiatherothrombotic, anti-leukemic, and tranquilizing effects (Khandekar et al. 2013, Rao 2021). The plant is characterized by obovate leaves that emit a camphor-like aroma and typically attains a height of 40 to 90 cm. The plant's axils are adorned with cymes of brilliant yellow flowers that are characterized by their sharp points (Lawrence 2017, Sinha et al. 2024).

The majority of the genus Corydalis (family Fumariaceae) is located in Eurasia (Coseri 2009). In east Asia, the plants of this genus have been employed as analgesic and anticancer agents (Author et al. 2010). Alkaloids are the most significant constituents responsible for its biological activities. Corydalis govaniana Wall. (CG) is a glabrous herb that is found in the Himalayas of Nepal, Pakistan, and India. It thrives in moist and shaded environments at an altitude of 2400-4800 meters. Syphilis, scrofula, cutaneous infections, diarrhoea, and dysentery have all been treated with the roots ethnographically (CSIR 1951, Mukhopadhyay et al. 1987). A variety of malignancies, including hepatitis, cirrhosis, ascites, amoebiasis, and liver cancer, have been effectively treated with plant extracts, pure compounds, and alkaloids from this genus in various species (Mukhopadhyay et al. 1987).

Conventional system of drug delivery has been modified and investigated to develop a system that is suitable for drug delivery. Conventional drug delivery system has several disadvantages such as first pass metabolism, frequent dosing, excessive excretion of drug. Nanotechnology is one of the innovative technologies that has been envisaged to avoid such demerits and improve bioavailability. It is anticipated that the utilization of nanosized carriers in the delivery of active ingredients will enhance the specificity and efficacy of the active ingredient, thereby reducing the incidence of reducing adverse effects and the dosage. Nanotechnology-driven active ingredient systems enable site-specific skin targeting, which may result in increased active ingredient retention at the target site (Lohani et al. 2014, Ghazwani et al. 2023a). Silver of nanoparticles are one the most nanoformulation. Silver nanoparticles (AgNPs) have garnered significant attention from researchers due to their diverse and remarkable applications across various fields. As one of the most promising nanomaterials, AgNPs play a crucial role in advancing the commercialization of silver-based industrial products. They are widely utilized in engineering, biomedical sciences, and agriculture (Anon n.d., Otsuka 2012, Bamsaoud et al. 2021). Numerous methods for synthesizing AgNPs have been developed, including chemical, physical, photochemical, and biological approaches (Vasileva Tsanova et al. 2011, Krishnaraj et al. 2012, El-Nour et al. 2016). Each method has its own advantages and limitations concerning cost, scalability,

particle size, and size distribution. However, chemical and physical methods often involve toxic substances, which limit their broader applications. Consequently, green synthesis approaches have emerged as a preferred alternative, offering a cost-effective and environmentally friendly solution that is better suited for large-scale production of nanoparticles (Mittal et al. 2013, Bamsaoud et al. 2021). In our study we have prepared and optimized drug loaded silver nanoparticles that are envisaged to act against human skin cancer cells. The formulation is studied for its antioxidant, in vitro release and ex vivo permeations. The penetration of drug loaded nanoparticles are also evaluated using Confocal Laser Scanning Microscopy (CLSM). Morphological evaluation is also done by Transmission Electron Microscopy (TEM) analysis.

MATERIAL AND METHOD

Materials

The aerial part (leaves) of Blumea lacera and Corydalis govaniana plant purchase from Universal Biotech Old Delhi, India. They were authenticated by Department of Botany Jamia Hamdard by Dr. Salik Noorani Khan (Reference no. BOT/09/2512). Various solvents like ether, methanol, distilled water etc. were provided by the institute and were of analytical grade.

Synthesis of drug loaded silver nanoparticles (BLCG-AgNPs)

Carefully measured extract mixture of Blumea lacera and Corydalis govaniana were combined with an aqueous 0.01 M AgNO₃ solution (20 ml) in a 1:1 ratio, using a high-speed magnetic stirrer at temperatures of 25 °C and 60 °C, respectively. Due to their excellent dielectric properties, alcohol and water were used as stabilizers for efficient microwave heating. The mixture was then exposed to microwave irradiation at a frequency of 2.45 GHz with a power of 600 Watts. The solution transitioned from a clear appearance to a dark brown colour, indicating the formation of silver nanoparticles. This colour change was initially observed visually and later confirmed using UV-Spectroscopy (200-600 nm). The silver nanoparticles were purified by centrifugation and subsequent washing with distilled water and acetone to remove water-soluble impurities. Finally, the drugloaded silver nanoparticles were lyophilized and stored for further analysis.

Optimization of drug loaded AgNPs.

The Box-Behnken Design (BBD) in the Design Expert software (Version 13, Stat-Ease, MN, USA) was employed to optimize BLCG-AgNP synthesis. This method systematically examined the effects of three factors at three levels: AgNO₃ concentration (mM, X₁), microwave power (Watt, X₂), and extract concentration (X₃), on the dependent variables, silver nanoparticle size (Y₁) and absorbance (Y₂) (Table 1). These independent variables were assessed at three levels: low (-), medium (0), and high (+), to determine the optimal conditions. A total of 17 experimental runs, including three central

points, were conducted to evaluate the influence of the independent variables (Table 1). Polynomial equations and response surface plots were used to analyze the effects of these factors. The models considered, including linear and quadratic, assessed the relationship

between the independent and dependent variables. The quadratic model was identified as the most suitable, as it effectively captured both individual and interactive effects of the variables on the dependent outcomes (Sultana et al. 2023).

Table 1. Variables and Levels of the Box Behnken design applied for the optimization of silver nanoparticles.

Independent Variables	Levels (Actual, coded)			
	-1	0	1	
X1 AgNO3 concentration in mM	6	9	12	
X2 Microwave power (Watt)	400	600	800	
X3 Extract concentration (mg)	5	10	15	
Dependent variables	Goals			
Y1 particle Size (nm)	Minimize			
Y2 Absorbance	Maximize			

Characterization of drug loaded AgNPs.

Particle size, Polydispersity Index and Zeta Potential

Malvern Zetasizer (Zetasizer Ver. 7.12, Malvern Instruments Ltd.) was used to analyze the average diameter of nanoparticles, PDI and Zeta Potential. Formulation was diluted before analysis and done in triplicate at 25 °C with 90° scattering angle.

Determination of Entrapment efficiency

Ultracentrifugation technique was the suitable method to determine the percent of drug entrapped in the vesicle. The optimized formulation was centrifuged (C-24 BL; Remi Instruments Ltd., Vasai, India) for 1 h at 10,000 rpm to segregate out lingering drug from the formulation. The supernatant was pipetted out and analysed by UV spectrophotometer (Ghazwani et al. 2023b).

Percentage of entrapment efficiency (%EE) was calculated by Eq. 1.

Where, C1 was initial drug concentration and C2 was the drug concentration separated in the supernatant.

Fourier Transform Infrared Spectroscopy

To check the interaction of BL and CG and the compatibility of the optimized BLCG-AgNPs, FTIR spectrophotometry has been performed. Samples were mixed with KBr in a ratio of 1:100 and spectra were recorded in the range of 4000–400 cm -1.

Transmission Electron Microscopy

The size of BLCG-AgNPs were determined using Transmission Electron Microscopy (TEM). A small amount of the formulation was dispersed in distilled water to prepare the sample. A carbon-coated grid was placed on a paraffin sheet, and a drop of the sample was applied to the grid, allowing the nanoparticles to adhere to the carbon substrate for 1 minute. Subsequently, a drop of phosphotungstate was added to the grid and left for 10 seconds. The excess solution was carefully removed using filter paper. The prepared sample was then analysed using a TEM instrument (CRYO-TEM (TALOS S), Thermo Scientific, USA)

In vitro drug release

The in vitro release study of BLCG-AgNPs was performed using the dialysis method to assess the release of BL and CG from the AgNP and their suspension. The BLCG-AgNPs and BLCG-suspension were placed in pre-treated and activated dialysis bags with a molecular weight cutoff of 12,000 Da, and the bag ends were securely tied. These dialysis bags were immersed in separate beakers containing 250 mL of phosphate buffer (pH 6.4) supplemented with 7% v/v propylene glycol and 25% v/v isopropyl alcohol, maintained at 37°C. The beakers were kept at this temperature using a thermostatically controlled digital magnetic stirrer set at a swirling speed of 100 rpm. At specific time intervals (0, 0.25, 0.5, 1, 2, 4, 12, and 24 hours), 1 mL samples were withdrawn and replaced with an equal volume of fresh PBS (pH 6.4). The withdrawn samples were analysed spectrophotometrically at 241 nm. Each experiment was conducted in triplicate to ensure reproducibility of results. Additionally, the release kinetics of BLCG were evaluated by fitting the release data to various kinetic models (Waheed et al. 2022).

Ex vivo permeation study



Mice skin was procured from Etsy, Mumbai, India for this study. The skin was cleaned with isopropyl alcohol to remove any adhering fat or hairs. It was then positioned between the donor and receptor compartments, with the stratum corneum facing the donor chamber. The receptor compartment was filled with 10 mL of a 7:3 v/v mixture of phosphate-buffered saline (pH 5.5) and isopropyl alcohol, which was continuously stirred at 600 rpm using a magnetic stirrer. BLCG-AgNPs at a concentration of 1 mg/mL were applied to the skin in the donor compartment. Aliquots of 1 mL were withdrawn at predetermined time intervals of 1, 2, 4, 6, 8, 12, and 24 hours. To maintain sink conditions, the receptor compartment was replenished with fresh buffer after each sample collection. The drug concentration in the samples was analysed using UV spectroscopy (Dudhipala et al. 2020).

Antioxidant activity

The antioxidant activity percentage (% AA) of BLCG-AgNPs, BL and CG dispersion was determined using the 2,2-Diphenyl-1-picrylhydrazyl (DPPH) free radical scavenging method. A 0.02% DPPH solution was prepared in ethanol. BLCG-AgNPs, BL and CG dispersion were diluted to concentrations ranging from $10-100 \,\mu\text{g/mL}$ from the stock solution (1 mg/mL).

To perform the assay, $500~\mu L$ of each concentration of BLCG-AgNPs, BL and CG dispersion was mixed with $125~\mu L$ of the DPPH solution and allowed to stand for 1 hour in the dark. A colour change from violet to colourless signified antioxidant activity. Absorbance (Abs) was measured at 517 nm using a UV-VIS spectrophotometer (DU 800; Beckman Coulter, Fullerton, CA, USA). A DPPH solution without BLCG-AgNPs, BL and CG dispersion served as the blank. The % AA was calculated using the following equation (Rahman et al. 2015, Ali et al. 2022).

$$\%AA = \frac{absorbance\ of\ control\ sample\ -\ absorbance\ of\ test\ sample}{absorbance\ of\ control\ sample}*100$$

Anticancer activity against skin cancer cell line by MTT Assay

The MTT Assay was employed to evaluate cell viability. Skin cancer cell line A431 cells (5×10^3) were seeded per well into 96-well plates containing 100 μ L of DMEM medium supplemented with 10% FBS and incubated at 37°C. Cells were treated with varying concentrations of the test compound ($10-500~\mu$ g/mL) for 24 hours. Doxorubicin ($10-500~\mu$ g/mL) was used as a positive control, while $100~\mu$ L of DMEM served as the negative control; wells without cells were treated as blanks.

After incubation in a humidified incubator with 5% CO₂ at 37°C for 48 hours, 20 μ L of 5 mg/mL MTT solution diluted in PBS was added to each well and incubated for an additional 4 hours. Subsequently, 100 μ L of 10% SDS in 0.01 M HCl was added to each well to dissolve the formazan crystals. The plates were covered with aluminium foil and placed in an incubator for 12 hours to ensure complete dissolution of the crystals. The quantity of formazan was determined by measuring the absorbance at 560 nm using a microplate reader (Mosmann 1983).

Stability studies

Stability of optimized BLCG-AgNPs were carried on the formulation samples stored at 25 °C and 4 °C for a period of 24 weeks. Particle size and %EE were determined to test the stability of the silver nanoparticles. Samples were withdrawn at 1, 4, 8, 12, 16, 20 and 24 weeks and estimated (Waheed et al. 2022).

Statistical analysis

The data will be expressed as mean \pm Standard deviation. Statistical differences between groups will be analysed using one-way Analysis of Variance (ANOVA) followed by Tukey post hock test/Student's t test (Agrawal et al. 2010).

RESULTS AND DISCUSSION

Response surface analysis by Design Expert- Box Behnken Design

Using Design Expert software (version 13), seventeen formulation runs—expected—were developed; the results are shown in Table 2. The quadratic model was found, using model summary analysis, to have the best fit for the two chosen responses. Fig.1. Shows three-dimensional graphs showing how the independent factors affect the responses Y1, and Y2. The expected R^2 values for this design were noted to match the modified R^2 values.

Table 2: Experimental trial with recorded response and associated anticipated response.

Independent Variables Dependent variables						
			Observed response Predicted res			response
X1	X2	X3	Y1	Y2	Y1	Y2
12	600	5	255.87	0.937	256.99	0.911
6	800	10	254.11	0.892	256.86	0.834
6	600	15	285.22	0.671	283.65	0.628
9	800	15	270.15	0.929	272.44	0.892
	1	X1 X2 12 600 6 800 6 600	X1 X2 X3 12 600 5 6 800 10 6 600 15	X1 X2 X3 Y1 12 600 5 255.87 6 800 10 254.11 6 600 15 285.22	X1 X2 X3 Y1 Y2 12 600 5 255.87 0.937 6 800 10 254.11 0.892 6 600 15 285.22 0.671	X1 X2 X3 Y1 Y2 Y1 12 600 5 255.87 0.937 256.99 6 800 10 254.11 0.892 256.86 6 600 15 285.22 0.671 283.65

luman Skin	JOURNAL OF RARE CARDIOVASCULAR DISEASES

5	6	400	10	115.21	0.736	117.32	0.749
6	9	400	5	86.32	0.775	85.88	0.788
7	9	600	10	153.76	0.932	155.90	0.953
8	9	400	15	148.11	1.23	150.24	1.45
9	9	600	10	154.98	0.551	155.64	0.582
10	12	600	15	224.87	0.701	227.32	0.694
11	12	400	10	179.91	0.932	180.33	0.899
12	9	600	10	166.84	0.951	168.93	0.972
13	9	600	10	151.22	0.563	150.21	0.536
14	6	600	5	80.31	0.632	82.33	0.691
15	12	800	10	255.81	0.571	255.52	0.552
16	9	600	10	139.55	1.32	140.76	1.42
17	9	800	5	180.22	0.913	180.89	0.938

Response Y1: effect of variables on particle size

Particle size: 153.27 + 22.70X1 + 53.84X2 + 40.70X3 – 15.75X1X2 – 58.98 X1X3 + 7.03 X2X3 + 44.18X12 + 3.81X22 + 14.12X32 17 runs generated by Box Behnken Design were experimentally run and gave vesicle size of range 82.33 nm to 283.65 nm. The quadratic equation showed that particle size increased with the enhancing the concentrations of AgNO3. The power of microwave also showed positive effect on the particle size. Similarly, more the drug concentration is added bigger is the particle size. The polynomial equation demonstrated a quadratic model with a F statistic of 1.26. The model terms were validated by a P-value below 0.05, indicating a noise probability of merely 0.01%. The optimal model was validated with a correlation coefficient (R2) of 0.9888, whereas the correlation coefficients for the anticipated and actual values were 0.9038 and 0.9744, respectively (Table 3). The proximity of real and anticipated coefficients indicates the model's robustness. The signal-to-noise ratio was determined to be 25.991, demonstrating adequate precision and suggesting that the model is dependable for particle measurement design.

The increase in the concentration of the both AgNO3 and BL and CG extract consecutively enhanced the particle size as they get incorporated in the layers of the nanoparticle resulting in broadening the size of the vesicles of the nanoparticle (Bamsaoud et al. 2021). As per the equation the involvement of the power of microwave with the concentration of AgNO3 (AC) and concentration of extract (BLCG) signify that power of microwave will still produce the positive effect on the size of the particle. These effects were observed to be well fitted in the analysis.

Response Y2: effect of variables on Absorbance

 $0.9286 + 0.0684X1 + 0.1454X2 + 0.1225X3 + 0.0518X1X2 + 0.1915\ X1X3 + 0.1870\ X2X3 - 0.0437X12 - 0.1797X22 + 0.0296X32$

According to the equation above, it was found that the concentration of AgNO3 has positive effect on the absorbance. As the concentration of AgNO3 increases the absorbance increases. The drug concentration also caused absorbance value to increase. Similarly, microwave power enhances the absorbance level of the nanoparticles as seen in Fig 1 depicting the 3D graph model. Similar effect was shown by Ghazwani et al. The proximity of real and anticipated coefficients indicates the model's robustness. The signal-to-noise ratio was determined to be 48.272, demonstrating adequate precision and suggesting that the model is dependable for absorbance (Ghazwani et al. 2023a).

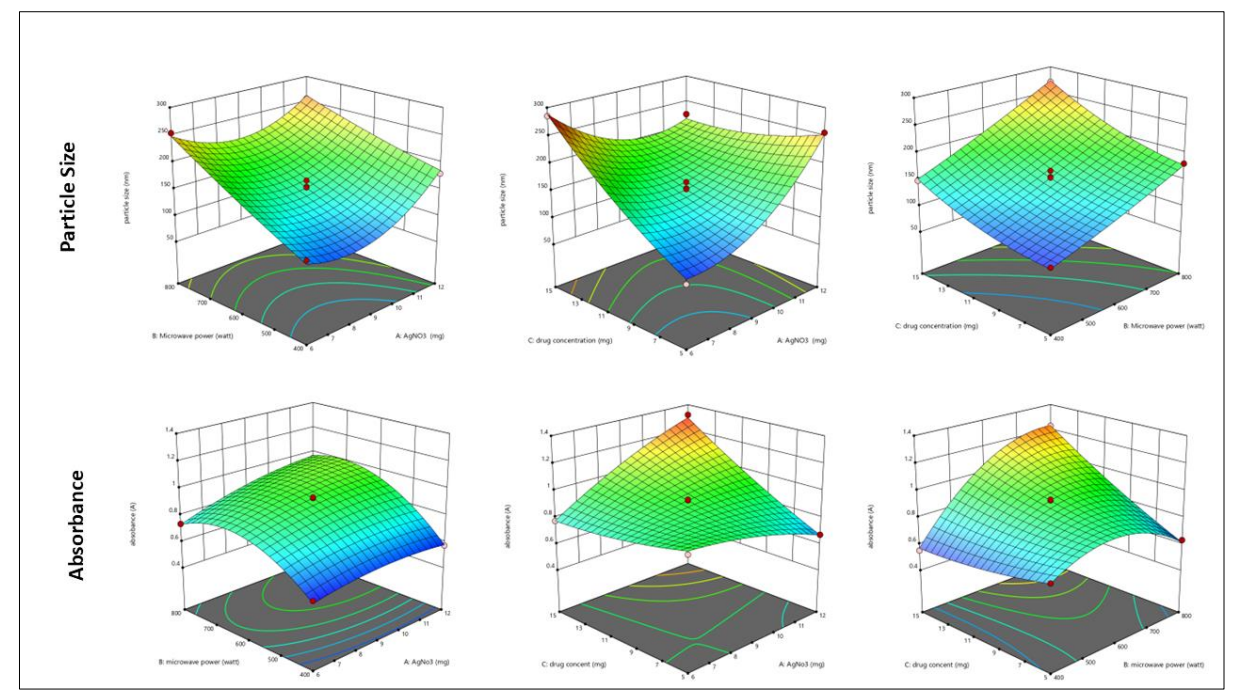


Figure 1: 3D graph depicting impact of independent variables on (A) particle size, (B) Absorbance

Table 3. The regression analysis of the three-level, three-factor BBD of silver nanoparticle and its output data.

Response	Model	R2	Adjusted R2	Predicted R2	P Value
Y1 Vesicle size	Quadratic	0.9888	0.9744	0.9038	0.3995
Y2 Absorbance	Quadratic	0.9963	0.9915	0.9465	0.0243

Validation of Experimental Design

The validity of the optimisation method was evaluated by comparing the predicted and experimental values. Table 2 contains the predicted values of each individual trial. The composition of the optimal formulation was determined by the results obtained from the responses. The predicted responses of the optimal formulation were also generated by the software, and these responses were subsequently compared to the optimised experimental formulation. The AgNO₃ concentration (mM, X_1), Microwave Power (Watt, X_2), and Extract concentration (X_3) were the components of the optimised formula that was obtained using BBD. The predicted responses for absorbance and particle size were 155.82 \pm 4.22 nm and 0.682, respectively, while the observed responses were 153.76 \pm 5.87 nm and 0.702. The results obtained indicated a strong correlation between the predicted and observed values. The optimized variable for the formulation was found to be 9 mg AgNO₃ concentration, 600 watt microwave power and 10 mg extract concentration. Therefore, the BLCG-AgNPs that were formulated with the most optimal composition were employed for subsequent research.

Characterization of optimized drug loaded AgNPs. Particle size, PDI, %EE

After synthesis, the zeta potential, polydispersity index, and mean particle size diameter were all measured using Malvern zetasizer (Malvern Instrument, Malvern, UK). 2 ml of AgNPs were administered in the quartz cell. Measurements were made thrice at a 90-degree angle to the light source. The optimized AgNPs were found to have size of 153.76 ± 5.87 nm and PdI 0.23 ± 0.042 (Fig. 2). The optimized BLCG-AgNPs have entrapment efficiency of $88.87 \pm 3.23\%$.

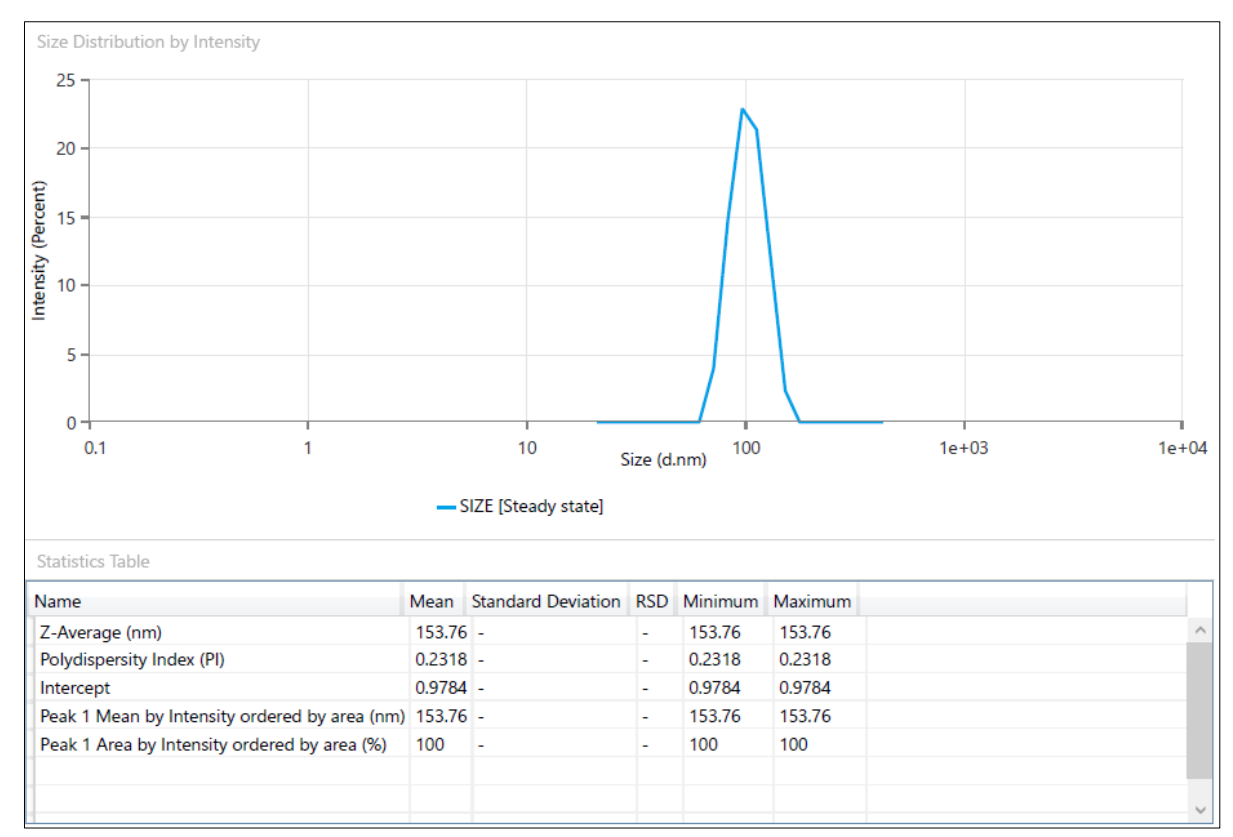


Figure 2: Particle size and PdI of optimised AgNPs

Zeta Potential

The greater electrostatic repulsion between nanoparticles with higher magnitudes of zeta potential results in more stable nanoparticles. The peak depicted in Figure 3 of the optimized BLCG-AgNPs zeta potential was found to be -23.961 \pm 4.66 mV, validating the formulation stability (Gunti et al. 2019).

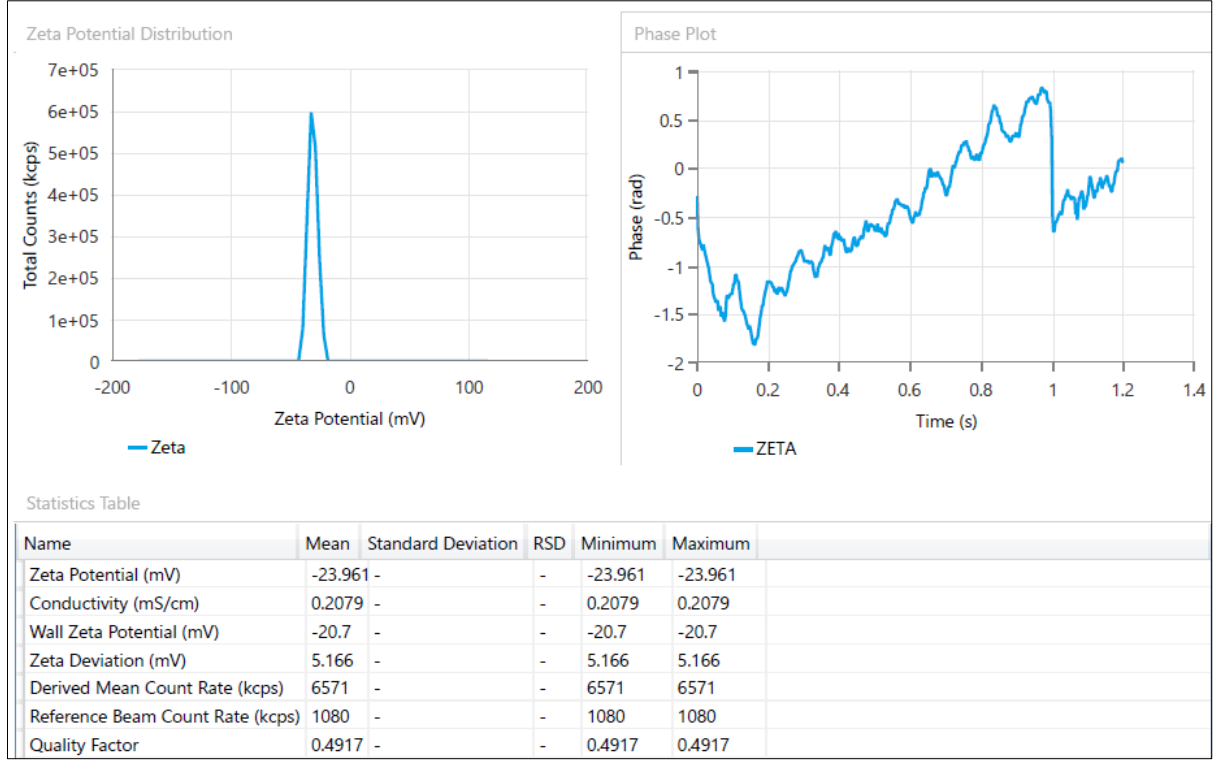


Figure 3: Zeta Potential of optimised AgNPs



FTIR

FTIR spectroscopy was established to understand the compatibility of the drugs and excipients used to formulate AgNPs. From the figure 4, the presence of characteristic peaks of BL and CG indicated that there is no any interaction taking place.

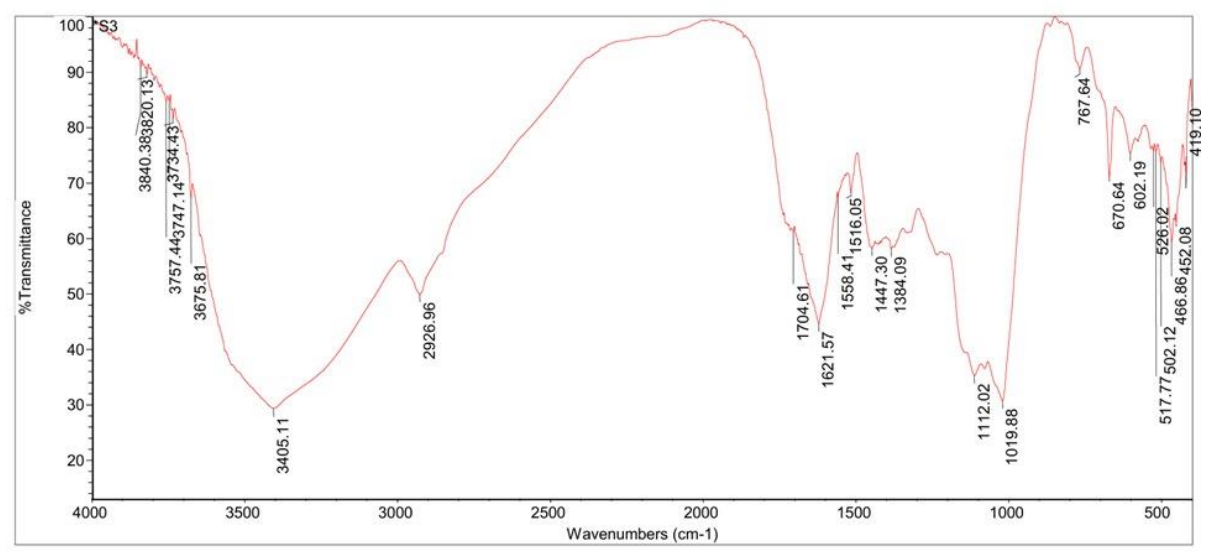


Figure 4: FTIR Spectroscopy of optimised AgNPs

TEM

The prepared BLCG-AgNPs were visualized using Transmission Electron microscopy (TEM) as shown in Fig 5. It was observed, the nanoparticles were spherically concealed and uniform. The particle size observed in TEM was corresponding to the results of particle size obtained by zeta sizer.

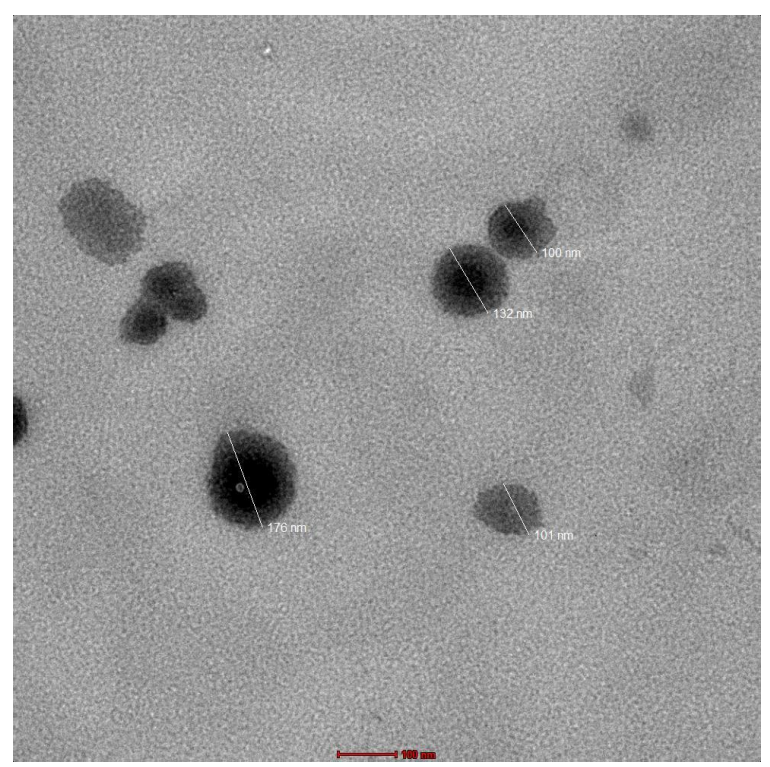


Figure 5: Optimized formulation TEM images (scale-100 nm)

In vitro drug release

To evaluate the release of Blumea lacera and Corydalis govaniana, the release behaviour of the prepared, optimized BLCG-AgNPs formulation and BLCG suspension was studied. The percentage of active ingredient released by the optimized BLCG-AgNPs was much higher, at $88.08 \pm 4.22\%$ and $77.84 \pm 5.23\%$ for BL and CG respectively, than that released by the BLCG-suspension, at $39.97 \pm 3.98\%$ and $48.69 \pm 4.45\%$ for BL and CG respectively (Figure 6). The graph shows that



there was a burst release at 2 h, which gradually reduces. While prolonged slow release increases therapeutic efficacy, initial fast release helps achieve therapeutic concentration. It was found that BLCG-AgNPs formulation results in a controlled release of the entrapped active ingredient over a period of 24 h. Several models, including the zero order, first order, Higuchi and Korsmeyer-Peppas models, were used to analyze the in vitro release data (Table 4.). Highest value of correlation coefficient (R2) was considered to be the best fid model. In the case of optimal BLCG-AgNPs, the Higuchi model was shown to have the highest correlation coefficient followed by the first-order model and the zero-order model shown in Table 3. The maximum value of the correlation coefficient (R2) was discovered for the optimized BLCG-AgNPs, establishing Higuchi's model as the best-fit model. The Korsmeyer-Peppas model revealed that the release of BLCG from the optimized BLCG-AgNPs follows non-fickian diffusion; the R2 and n values were shown in table 4 for both the drugs (Alam et al. 2023, Ghazwani et al. 2023a).

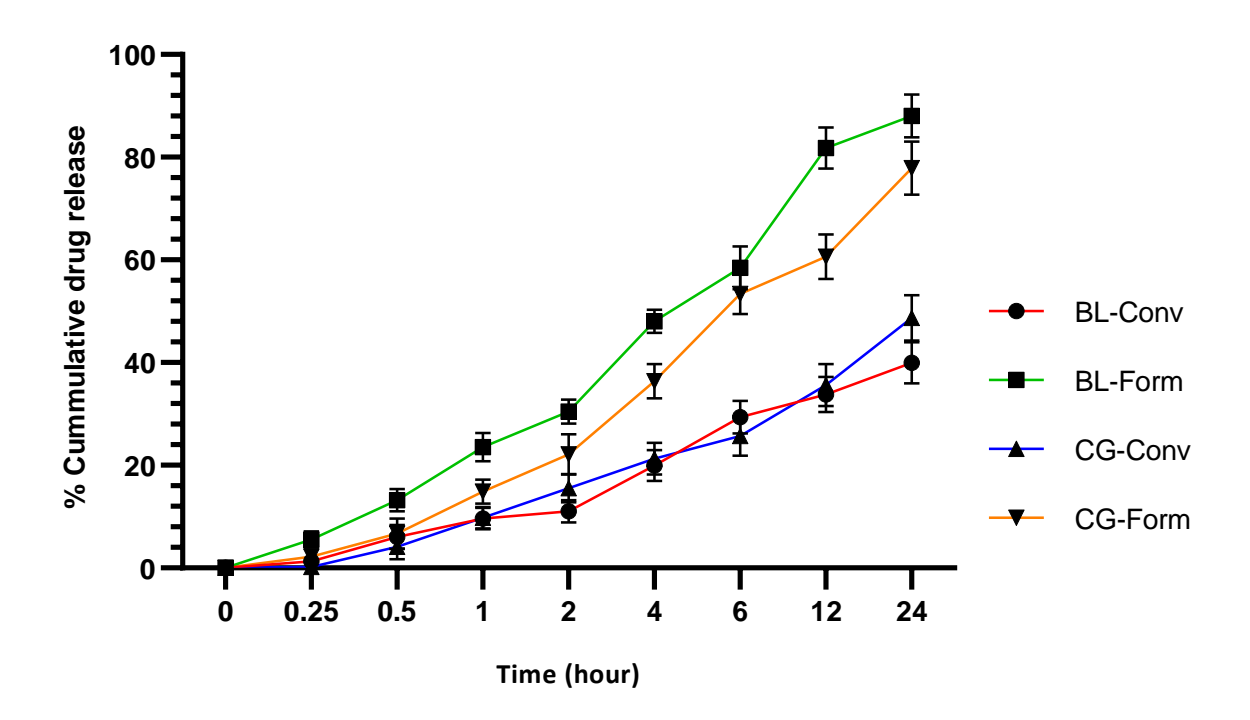


Figure 6: In vitro drug release study

Table 4. Release Kinetics of BLCG-AgNPs

Drug Loaded	Zero order	First order	Korsmeyer-peppas model	Higuchi model
Transferosomes	model (R2)	model (R2)	(R2 and n)	(R2)
BL	0.785	0.9263	0.9462, 0.3666	0.9407
CG	0.8168	0.939	0.9304, 0.5666	0.9546

Ex Vivo permeation study

The study on drug permeation through rat skin revealed a notable difference in performance between the conventional BLCG suspension and the optimized BLCG-AgNP formulation. The conventional suspension achieved a drug permeation of $40.98 \pm 3.99\%$ for BL and $38.99 \pm 3.11\%$ for CG, highlighting its limited efficiency in crossing the skin barrier. In contrast, the optimized BLCG-AgNP formulation significantly improved drug permeation, achieving $75.08 \pm 4.34\%$ for BL and $76.49 \pm 3.44\%$ for CG, as illustrated in Figure 7. This enhanced permeation can be attributed to the unique properties of silver nanoparticles (AgNPs). The lipid interaction within the skin barrier and the presence of phospholipids in the AgNP formulation facilitate greater compatibility and integration, thereby improving drug transport. Furthermore, the small size of AgNPs enables them to penetrate the skin more effectively, including through hair follicles, which serve as additional pathways for deeper delivery. This demonstrates the superior capability of AgNPs as carriers in transdermal drug delivery systems (Trbojevich et al. 2016).

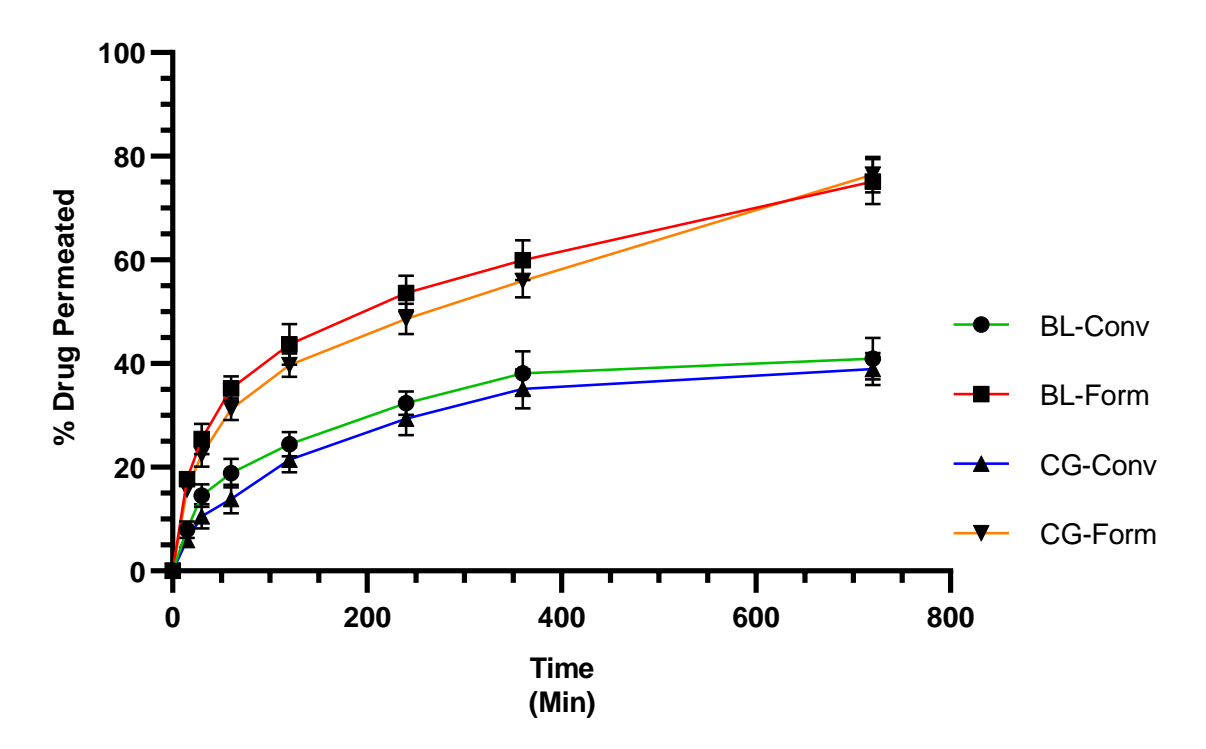


Figure 7: Ex Vivo skin permeation study

Antioxidant activity

Six different concentrations (50, 100, 150, 200, 250, and 300 μ g/ml) of the drug samples exhibited varying percentages of inhibition, with the scavenging activity increasing in a concentration-dependent manner (Fig.8). At the highest concentration of 300 μ g/mL, the samples demonstrated the most potent antioxidant activity. Among these, ascorbic acid (AA) displayed the highest activity (94.37 \pm 3.12%), followed by BLCG-AgNPs (1:1) (89.28 \pm 2.86%), BL (83.22 \pm 2.65%), and CG (79.76 \pm 2.11%). Notably, the radical scavenging activity of the BLCG-AgNPs formulation at 300 μ g/mL was comparable to that of AA at the same concentration (Fig. 8). This enhanced activity in the drug-loaded formulation may be attributed to improved solubility and dispersion achieved through nanoparticle formulation. These results confirm that the antioxidant properties of the drugs were preserved within the formulation. The concentration required for 50% inhibition of DPPH (IC50 value) and the percentages of inhibition at various concentrations are detailed in Supplementary Table 5 and Fig. 8. Notably, lower IC50 values indicate greater antioxidant activity. The IC50 values for BL and CG were 45.83 \pm 2.22 μ g/mL and 48.23 \pm 1.89 μ g/mL, respectively.

Blumea lacera and Corydalis govaniana solution in the ratio 1:1 was selected as it was found to be the best combination ratio having the lowest IC50 compared to the other ratios. The CI for the selected ratio of drugs was 0.629, i.e., lesser than 1, and confirms the synergistic effect of drugs when combined (1:1).

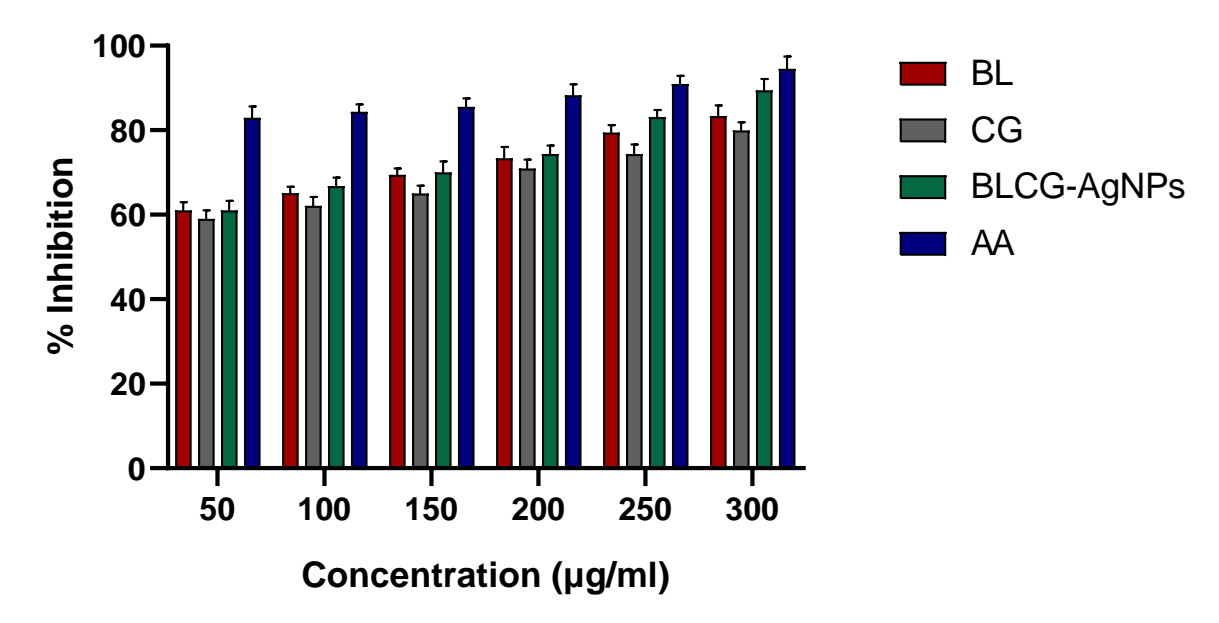


Figure 8: DPPH Assay-Percentage Inhibition by BL, CG, BLCG-AgNPs and AA

Table 5: DPPH free radical scavenging activity (517 nm)

		Half inhibition concentration in different
S. No.	Sample	extracts
		[IC50 (µg/mL)]
1	Blumea lacera extract	45.83
2	Corydalis govaniana extract	48.23
3	BL and CG loaded silver nanoparticle	66.90
4	Standard Ascorbic Acid	54.11

Anticancer activity against skin cancer cell line by MTT Assay

The cytotoxic potential of Blumea lacera and Corydalis govaniana phytoconstituents were evaluated against A431 skin cancer cell lines using the MTT assay (Figure 9). Blumea lacera demonstrated an IC₅₀ value of 416.80 μg/mL, indicating moderate cytotoxicity, while Corydalis govaniana exhibited a stronger effect with an IC₅₀ value of 248.60 μg/mL. Based on these findings, it is hypothesized that combining these two phytoconstituents could result in a synergistic effect, potentially enhancing their overall cytotoxic efficacy against A431 cells.

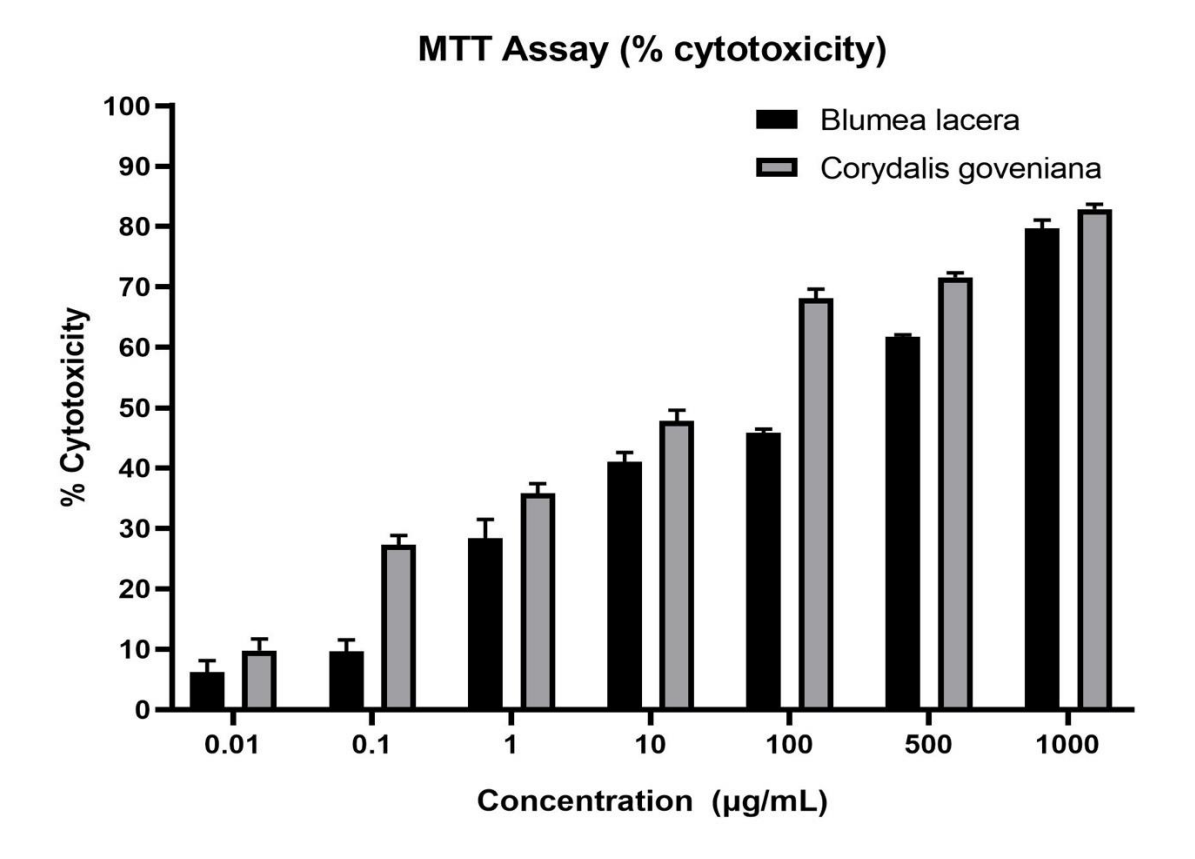


Figure 9: Percentage cytotoxicity of Blumea lacera and Corydalis govaniana phytoconstituents against A431 skin cancer cell lines at varying concentrations, as determined by the MTT Assay. Data represent mean \pm standard deviation from three independent experiments.

Stability studies

A study of the AgNPs stability was performed to determine how long it is expected to remain stable after preparation. The study showed that BLCG-AgNPs does not exhibit any phase separation and conforms to all requirements with respect to particle size and %EE (Table 6). It was discovered that BLCG-AgNPs formulations was best when kept in a cool, dry environment.

Table 6: Stability studies of optimized BLCG-AgNPs								
Parameters for		Initial	1 Month		3 Month			
evaluation			4 ± 2 °C	25 ± 2	4 ± 2	25 ± 2	4 ± 2 °C	25 ± 2
				$^{\circ}\text{C}/~60~\pm$	$^{\circ}\mathrm{C}$	$^{\circ}\text{C}/~60~\pm$		$^{\circ}\text{C}/~60~\pm$
				5% RH		5% RH		5% RH
Physical appearan	ce	No chang	e in physica	l appearance	е			
Phase separation		No phase	No phase separation					
particle size (nm)								
%EE		88.87 ±	86.12 ±	85.38 ±	85.01 ±	83.36 ±	82.22 ±	81.81 ±
		3.23%	2.45%	3.67%	1.26%	4.19%	2.87%	2.11%

CONCLUSION

The microwave-assisted synthesis has proven to be an efficient technique to obtain BL-CG loaded silver nanoparticles (BLCG-AgNPs). The formulation was optimised with the Box-Behnken Design (BBD), taking into account both independent and dependent variables to get optimal particle size and absorbance. In vitro release study indicated that BLCG-AgNPs released almost double the active components in comparison to conventional BL and CG suspension. Ex vivo

permeation experiments demonstrated that BLCG-AgNPs gel infiltrated the dermis and epidermis more effectively than conventional formulations, suggesting its suitability for topical applications necessitating improved penetration and sustained retention of active components. Furthermore, the BLCG-AgNPs formulation demonstrated superior antioxidant activity and improved UV protection. The cytotoxic ability of BLCG against malignant cells was validated using the MTT Assay. The promising results indicate that BLCG-



AgNPs may function as an effective topical delivery mechanism for BL and CG, especially in the treatment of UVB-induced skin damage. Nonetheless, additional preclinical and clinical investigations, in conjunction with dermatological assessments, are required to ascertain the formulation's safety and efficacy, with the objective of achieving a favourable low-risk/high-benefit ratio in comparison to current high-risk/low-benefit alternatives.

REFERENCE

- 1. Afaq F (2011) Natural agents: Cellular and molecular mechanisms of photoprotection. Archives of Biochemistry and Biophysics 508: 144–151.
 - https://doi.org/10.1016/j.abb.2010.12.007
- 2. Agrawal A, Verma P, Goyal PK (2010) Chemomodulatory effects of Aegle marmelos against DMBA-induced skin tumorigenesis in swiss albino mice. Asian Pacific Journal of Cancer Prevention 11: 1311–1314.
- 3. Alam A, Foudah AI, Alqarni MH, Yusufoglu HS (2023) Microwave-assisted and chemically tailored chlorogenic acid-functionalized silver nanoparticles of Citrus sinensis in gel matrix aiding QbD design for the treatment of acne. Journal of Cosmetic Dermatology 22: 1613–1627. https://doi.org/10.1111/jocd.15611
- Ali A, Aqil M, Imam SS, Ahad A, Parveen A, Qadir A, Ali MH, Akhtar M (2022) Formulation and evaluation of embelin loaded nanoliposomes: Optimization, in vitro and ex vivo evaluation. Journal of Drug Delivery Science and Technology 72: 103414. https://doi.org/10.1016/j.jddst.2022.103414
- 5. Anon Intrinsic therapeutic applications of noble metal nanoparticles: past, present and future. pubs.rsc.org RR Arvizo, S Bhattacharyya, RA Kudgus, K Giri, R Bhattacharya, P Mukherjee Chemical Society Reviews, 2012•pubs.rsc.org.
- Anon Melanoma Skin Cancer Statistics | American Cancer Society. Available from: https://www.cancer.org/cancer/types/melanom a-skin-cancer/about/key-statistics.html (January 7, 2025b).
- Apalla Z, Lallas A, Sotiriou E, Lazaridou E, Ioannides D (2017) Epidemiological trends in skin cancer. Dermatology Practical & Conceptual 7. https://doi.org/10.5826/dpc.0702A01
- 8. Author C, Simanjuntak P, Djamil R, Lelly Heffen W (2010) Apoptosis of human breast cancer cells induced by ethylacetate extracts of propolis. academia.edu JS Sawah, jlsp Kav American Journal of Biochemistry and Biotechnology, 2010•academia.edu 6: 84–88.
- 9. Bamsaoud SF, Basuliman MM, Bin-Hameed EA, Balakhm SM, Alkalali AS (2021) The effect of volume and concentration of AgNO3 aqueous solutions on silver nanoparticles

- synthesized using Ziziphus Spina–Christi leaf extract and their antibacterial activity. Journal of Physics: Conference Series 1900: 012005. https://doi.org/10.1088/1742-6596/1900/1/012005
- 10. Cohen JL (2010) Actinic keratosis treatment as a key component of preventive strategies for nonmelanoma skin cancer. Journal of Clinical and Aesthetic Dermatology 3: 39–44.
- 11. Coseri S (2009) Natural Products and their Analogues as Efficient Anticancer Drugs. Mini-Reviews in Medicinal Chemistry 9: 560–571. https://doi.org/10.2174/138955709788167592
- 12. CSIR (1951) CSIR Annual report 1950-51.
- 13. Dudhipala N, Phasha Mohammed R, Adel Ali Youssef A, Banala N (2020) Effect of lipid and edge activator concentration on development of aceclofenac-loaded transfersomes gel for transdermal application: in vitro and ex vivo skin permeation. Drug Development and Industrial Pharmacy 0: 1334–1344. https://doi.org/10.1080/03639045.2020.178806
- 14. El-Nour KMA, Hassan AM, Abdulwahid OA (2016) Silver and zinc oxide nanoparticles as potential weapons for enhancement of antibiotics activity against multi drug resistant microorganisms. European Journal of Chemistry 7: 290–297. https://doi.org/10.5155/eurjchem.7.3.290-297.1438
- 15. Ferlay J, Colombet M, Soerjomataram I, Mathers C, Parkin DM, Piñeros M, Znaor A, Bray F (2018) Estimating the global cancer incidence and mortality in 2018: Globocan sources and methods. Wiley Online Library J Ferlay, M Colombet, I Soerjomataram, C Mathers, DM Parkin, M Piñeros, A Znaor, F Bray International journal of cancer, 2019•Wiley Online Library 144: 1941–1953. https://doi.org/10.1002/ijc.31937
- 16. Ghazwani M, Hani U, Alqarni MH, Alam A (2023a) Development and Characterization of Methyl-Anthranilate-Loaded Silver Nanoparticles: A Phytocosmetic Sunscreen Gel for UV Protection. Pharmaceutics 2023, Vol. 15, Page 1434 15: 1434. https://doi.org/10.3390/ pharmaceutics 15051434
- 17. Ghazwani M, Hani U, Alam A, Alqarni MH (2023b) Quality-by-Design-Assisted Optimization of Carvacrol Oil-Loaded Niosomal Gel for Anti-Inflammatory Efficacy by Topical Route. Gels 2023, Vol. 9, Page 401 9: 401. https://doi.org/10.3390/gels9050401
- 18. Gunti L, Dass RS, Kalagatur NK (2019) Phytofabrication of Selenium Nanoparticles From Emblica officinalis Fruit Extract and Exploring Its Biopotential Applications: Antioxidant, Antimicrobial, and



- Biocompatibility. Frontiers in microbiology 10. https://doi.org/10.3389/ fmicb.2019.00931
- 19. Khandekar U, Tippat S, Ghongade R (2013) Investigation on antioxidant, Antimicrobial and phytochemical profile of Blumea lacera leaf International Journal of Biological & Pharmaceutical Research investigation on antioxidant, Antimicrobial and phytochemical profile of Blumea lacera leaf. Article in International Journal of Biological & Pharmaceutical Research 4.
- Krishnaraj C, Jagan EG, Ramachandran R, Abirami SM, Mohan N, Kalaichelvan PT (2012) Effect of biologically synthesized silver nanoparticles on Bacopa monnieri (Linn.) Wettst. plant growth metabolism. Elsevier 47: 651–658. https://doi.org/10.1016/j.procbio.2012.01.006
- 21. Lawrence G (2017) Taxonomy of vascular plants.
- Lohani A, Verma A, Joshi H, Yadav N, Karki N (2014) Nanotechnology-Based Cosmeceuticals. International Scholarly Research Notices 2014: 843687. https://doi.org/10.1155/2014/843687
- 23. Mangione CM, Barry MJ, Nicholson WK, Chelmow D, Coker TR, Davis EM, Donahue KE, Jaén CR, Kubik M, Li L, Ogedegbe G, Rao G, Ruiz JM, Stevermer J, Tsevat J, Underwood SM, Wong JB (2023) Screening for Skin Cancer: US Preventive Services Task Force Recommendation Statement. jama 329: 1290– 1295. https://doi.org/10.1001/jama.2023.4342
- Mittal AK, Chisti Y, Banerjee UC (2013) Synthesis of metallic nanoparticles using plant extracts. Biotechnology Advances 31: 346– 356. https://doi.org/10.1016/j.biotechadv.2013.01.0
 - https://doi.org/10.1016/j.biotechadv.2013.01.0 03
- Mokhtari RB, Homayouni TS, Baluch N, Morgatskaya E, Kumar S, Das B, Yeger H (2017) Combination therapy in combating cancer. Oncotarget 8: 38022–38043. https://doi.org/10.18632/oncotarget.16723
- Mosmann T (1983) Rapid colorimetric assay for cellular growth and survival: Application to proliferation and cytotoxicity assays. Journal of Immunological Methods 65: 55–63. https://doi.org/10.1016/0022-1759(83)90303-4
- Mukhopadhyay S, Banerjee SK, Atal CK, Lin LJ, Cordell GA (1987) Alkaloids of corydalis govaniana. Journal of Natural Products 50: 270–272. https://doi.org/10.1021/np50050A033
- Otsuka H (2012) PEGylated Nanoparticles for Biological and Pharmaceutical Applications. In: Electrical Phenomena at Interfaces and Biointerfaces: Fundamentals and Applications in Nano-, Bio-, and Environmental Sciences., 815–838.

- https://doi.org/10.1002/9781118135440.ch47
- 29. Rahman MM, Islam MB, Biswas M, Khurshid Alam AHM (2015) In vitro antioxidant and free radical scavenging activity of different parts of Tabebuia pallida growing in Bangladesh. Springer MM Rahman, MB Islam, M Biswas, AHM Khurshid Alam BMC research notes, 2015•Springer 8: 621. https://doi.org/10.1186/s13104-015-1618-6
- 30. Rao AM (2021) In vitro antioxidant and anticancer activity of Blumea lacera leaf extract. Journal of Biotech Research 12: 168–176.
- 31. Sinha D, Banerjee S, Majgaonkar A, Pomila, Datta S, Chanda S, Chatterjee M, Bhattacharya R, Maurya AK (2024) Blumea lacera (Burm.f.) DC: A review on ethnobotany, phytochemistry, ancient medicinal and pharmacological Uses. Plant Science Today 11: 161–174. https://doi.org/10.14719/pst.2903
- 32. Sohrabi M, Babaei Z, Haghpanah V, Larijani B, Abbasi A, Mahdavi M (2022) Recent advances in gene therapy-based cancer monotherapy and synergistic bimodal therapy using conversion nanoparticles: Structural and biological aspects. Biomedicine and Pharmacotherapy 156. https://doi.org/10.1016/j.biopha.2022.113872
- 33. Sultana N, Ali A, Waheed A, Jabi B, Yaqub khan M, Mujeeb M, Sultana Y, Aqil M (2023) Dissolving microneedle transdermal patch loaded with Risedronate sodium and Ursolic acid bipartite nanotransfersomes to combat osteoporosis: Optimization, characterization, in vitro and ex vivo assessment. International Journal of Pharmaceutics 644. https://doi.org/10.1016/j.ijpharm.2023.123335
- 34. Trbojevich RA, Fernandez A, Watanabe F, Mustafa T, Bryant MS (2016) Comparative study of silver nanoparticle permeation using Side-bi-Side and Franz diffusion cells. Journal of Nanoparticle Research 18: 1–12. https://doi.org/10.1007/s11051-016-3363-8
- 35. Vasileva Tsanova P, Karadjova I, Vasileva P, Donkova B, Karadjova I, Dushkin C (2011) Synthesis of starch-stabilized silver nanoparticles and their application as a surface plasmon resonance-based sensor of hydrogen peroxide. Elsevier P Vasileva, B Donkova, I Karadjova, C Dushkin Colloids and Surfaces A: Physicochemical and Engineering Aspects, 2011•Elsevier 382: 203–210. https://doi.org/10.1016/j.colsurfa.2010.11.060
- 36. Waheed A, Zameer S, Sultana N, Ali A, Aqil M, Sultana Y, Iqbal Z (2022) Engineering of QbD driven and ultrasonically shaped lyotropic liquid crystalline nanoparticles for Apigenin in the management of skin cancer. European Journal of Pharmaceutics and Biopharmaceutics 180: 269–280.



- https://doi.org/10.1016/j.ejpb.2022.10.015
- 37. Yap TA, Omlin A, De Bono JS (2013) Development of therapeutic combinations targeting major cancer signaling pathways. Journal of Clinical Oncology 31: 1592–1605. https://doi.org/10.1200/jco.2011.37.6418